Can the Methoxyradical CH_3O Act as Sink for Cl and ClO in the Atmosphere?

Melanie Schnell,[†,‡] Max Mühlhäuser,[†,§] and Sigrid D. Peyerimhoff*[,†]

Institut für Physikalische und Theoretische Chemie der Universität Bonn, Wegelerstrasse 12, D-53115 Bonn, Germany, Institut für Physikalische Chemie und Elektrochemie der Universität Hannover, Callinstrasse 3-3a, D-30167 Hannover, Germany, and Verfahrens- und Umwelttechnik (FH), Management Center, Egger-Lienz-Strasse 120, A-6020 Innsbruck, Austria

Received: August 19, 2003; In Final Form: November 5, 2003

Several reaction pathways on the potential energy surface for the reaction $CH_3O + ClO$ are investigated using ab intio methods. As a result we find two reaction pathways to be most probable: (i) the formation of $CH_2O + HOCl$ via hydrogen abstraction from the methoxy radical and (ii) the formation of the low-lying adduct CH_3OOCl. The other adduct CH_3OClO is calculated to lie about 25 kcal/mol higher in energy than CH_3OOCl. CH_3OOCl can be considered to be a sink for Cl and ClO radicals on the ground-state surface. We have also performed MRD-CI calculations for the excited states of CH_3OOCl and CH_3OClO to study their photochemistry. In CH_3OOCl we calculated a strong transition (11a → 14a) at 4.80 eV corresponding to a σ(Cl−O)−σ*(Cl−O) excitation. We find all low-lying excited singlet and triplet states in the energy range between 2.5 and 5.5 eV to be highly repulsive toward Cl−O and O−O cleavage, and thus photodissociation pathways forming the reactive radicals Cl and ClO from CH_3OOCl are very probable.

Introduction

Methoxy radicals are known to be important intermediates in the oxidation mechanism of hydrocarbons either in combustion processes or in atmospheric chemistry. One important question is whether they can react with radicals such as ClO, which is known to play an important role in the ozone depletion cycle in the atmosphere under formation of stable adducts, so that they can act as a sink for aggressive radicals in the atmosphere.

Experimental studies concerning the kinetics of the methoxy radical CH_3O with reactive species, mostly radicals such as NO_x or O_2, are known.[1,2,] Daele et al.[3] have published an extensive experimental study on the kinetics of the reactions of CH_3O with Cl and ClO. For the reaction

$$CH_3O + ClO \rightarrow \text{products} \qquad (1)$$

Daele et al.[3] measured a rate constant of $k_1 = (2.3 \pm 0.3) \times 10^{-11}$ cm^3 molecule^{-1} s^{-1}, with a pure first-order decay of CH_3O. They suggested a reaction mechanism for reaction 1 via two exothermic channels:

$$CH_3O + ClO \rightarrow CH_2O + HOCl \quad \Delta H = -303 \text{ kJ mol}^{-1} \qquad (2)$$

$$CH_3O + ClO \rightarrow CH_2O_2 + HCl \quad \Delta H = -23 \text{ kJ mol}^{-1} \qquad (2a)$$

However, in this experimental study it was possible to clearly identify only HOCl as a reaction product. Neither CH_2O, HCl, nor the unstable radical CH_2O_2 could be detected. Thus they suggested channel (2) to be the major reaction.

On the other hand, the direct addition of both species leads to the adducts CH_3OOCl and CH_3OClO which could also be energetically stable. For example experimental and theoretical studies have shown that for the related systems CH_3O+Cl and CH_3O_2+Cl formation of the adduct methylhypochlorite CH_3-OCl is a dominant reaction pathway.[4,5] Thus, to clarify the major products of reaction 1, several different reaction pathways for the ground-state surface have to be investigated. Because of its atmospheric importance and the uncertainties about the reaction products in the experimental study of Daele et al.,[3] we decided to study several pathways on the ground-state potential energy surface of this system in detail. One aim in this investigation is to identify the competitive reactions and to evaluate the importance of the reaction channels (2) and (2a).

In addition, it is also important to consider the photochemistry of the system in the atmosphere. Thus an investigation of the excited states can give a key about the role of the species as a possible sink for aggressive radicals in atmospheric chemistry. In this study we will especially concentrate on the adducts CH_3-$OOCl$ and CH_3OClO of the system CH_3O and ClO which are expected to be energetically low-lying. Until now nothing is known about the spectroscopic behavior of these molecules. But it is obvious that photodissociation into reactive chlorine species such as Cl and ClO could be possible. Therefore we have performed multireference configuration interaction calculations (MRD-CI) to investigate the electronic absorption spectra of CH_3OOCl and CH_3OClO and their photodissociative behavior. The results should be also a guide for future spectroscopic and photochemical experiments.

After a brief introduction of computational techniques given in section 2, we will present in section 3 the results obtained for the different reaction pathways of the $CH_3O + ClO$ system and will discuss the calculated electronic absorption spectra of CH_3OOCl and CH_3OClO. In section 4 we will present the results of the photodissociation studies for CH_3OOCl, and finally, in section 5, conclusions will be summarized.

* Corresponding author. E-mail: unt000@uni-bonn.de
[†] Universität Bonn.
[‡] Universität Hannover.
[§] Verfahrens- und Umwelttechnik.

10.1021/jp030988u CCC: $27.50
Published on Web 01/24/2004

2. Computational Techniques

As starting points of our investigation we have fully optimized the geometries of the mimima and transition states of the CH_3O + ClO system using the DFT method with the hybrid functional B3LYP (6-311G* basis set). This procedure is justified since it is widely known, and we have explicitly shown in a recent paper[6] about the related system CH_3O + Cl, that reliable equilibrium geometries are already obtained at the B3LYP/6-31G* level. These DFT calculations have been performed using the Gaussian 98 series of programs.[7] Harmonic vibrational frequencies were calculated (B3LYP/6-311G*) to characterize the nature of the stationary points on the potential energy surface.

Based on these results we have performed singles and doubles coupled cluster calculations with perturbative inclusion of connected triple excitations using the MOLPRO 2000 program package.[8] The relative stability between these two isomers was obtained from single-point CCSD(T) calculations. We used the correlation-consistent triple-ζ basis set of Dunning[9] augmented by two d- and one f-polarization functions for the heavier atoms (cc-pVTZ). Zero point energies have also been taken into account.

For the calculation of excited states, the basis set was enlarged by an s-Rydberg function located at the carbon and a negative ion p-function for the chlorine (cc-p-VTZ+sp). The exponents taken are $\alpha_r(C) = 0.023$ and $\alpha_r(Cl) = 0.049$. A smaller polarized cc-pVDZ+sp basis set of double-ζ quality[9] with exponents $\alpha_d(C) = 0.55$, $\alpha_d(O) = 1.185$, $\alpha_d(Cl) = 0.60$ and the same s(C) and p(Cl) exponents as for the cc-pVTZ+sp basis was also used, and results show small changes in excitation energies and transition probabilities for the excited states examined in this work. These basis sets are flexible with respect to polarization and electron correlation, and are considered to be fairly balanced for all states treated, as we have shown in previous studies.[6,10]

The computations of the electronically excited states were performed with the multireference single and double excitation configuration interaction method MRD-CI implemented in the DIESEL program.[11] We used the recently completed[12] version 1.16 in which an automatic selection of reference configurations is carried out with a summation threshold. We used a summation threshold of 0.85 for the cc-pVDZ+sp calculations and of 0.82 for the cc-pVTZ+sp calculations, which means that the sum of the squared coefficients of all reference configurations selected for each state (root) is above 0.85 (0.82). The set of reference configurations per irreducible representation (IRREP) was in the range between 15 and 17 for both molecules. An analysis of the molecular orbitals (MO) involved in these selected reference configurations justified the prior choice of treating 26 electrons as active while keeping the remaining electrons in doubly occupied orbitals (frozen).

From this set of reference configurations (mains), all single and double excitations in the form of configuration state functions (CSFs) are generated. From this set, all configurations with an energy contribution $\Delta E(T)$ above a given threshold T were selected, i.e., the contribution of a configuration larger than this value relative to the energy of the reference set is included in the final wave function. A selection threshold of $T = 10^{-7}$ hartree was used. The effect of those configurations, which contribute less than $T = 10^{-7}$ hartree, is accounted for in the energy computation (E(MRD-CI)) by a perturbative technique. For a brief summary of the λ-extrapolation, see, for example, ref 13. The contribution of higher excitations is estimated by applying a generalized Langhoff−Davidson correction formula $E(MRD\text{-}CI+Q) = E(MRD\text{-}CI) - (1-c_0^2)$ [E(ref) − E(MRD-CI)]/ c_0^2, where c_0^2 is the sum of squared coefficients of the reference species in the total CI wave function and E(ref) is the energy of the reference configurations.

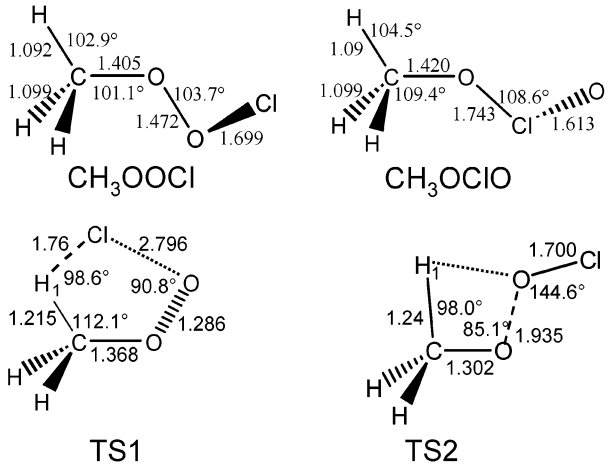

Figure 1. Optimized equilibrium geometries of CH_3OOCl, CH_3OClO, and the transition states (B3LYP/6-311G*). Bond lengths are given in Å, bond angles in degrees.

We examined the lower lying excited states of the molecules with both basis sets. The number of selected configurations in the MRD-CI space was of the order of 1.2 million (cc-pVDZ+sp) to 1.5 million (cc-pVTZ+sp). The number of configuration state functions (CSF) directly included in the energy calculations are as large as 4.5 million (cc-pVDZ+sp) and 6.8 million (cc-pVTZ+sp), so that transition energies of the examined energy region below 8 eV should be obtained with an error margin below 0.3 eV for both species.

Two models were adopted for the potential energy curves of CH_3OOCl: one was changing the O−Cl bond length stepwise in the range from 1.699 Å to 10 Å forming the dissociation products CH_3O_2 and Cl, while all other geometrical parameters were optimized. For this relaxation we used the more economic density functional method B3LYP as implemented in the Gaussian 98 program package[7] instead of CCSD(T). In the second model, the potential energy curve is obtained by elongating the O−O bond length from 1.405 Å to 10 Å under formation of CH_3O and ClO. Again, all other bond lengths and angles were optimized. We examined the lowest eleven states of CH_3OOCl for the dissociation via Cl−O elongation and the lowest nine states for O−O cleavage using the smaller cc-pVDZ+sp basis set.

3. Results and Discussion

In Figure 1 the equilibrium geometries of the adducts CH_3OOCl and CH_3OClO and the transition states calculated at the B3LYP/6-311G* level are shown. For the adducts CH_3OOCl and CH_3OClO, as well as for the transition states in the reaction of CH_3O and ClO, the harmonic vibrational frequencies are given in Table 1. As can be seen, we have calculated one imaginary frequency for TS1 and TS2, characterizing them as first-order saddle points.

In earlier work[14] the equilibrium geometries of CH_3OOCl and CH_3OClO have been calculated to be asymmetric with the OOCl− and the OClO− group rotated out of the symmetry plane of the molecule (gauche conformation). To investigate the equilibrium geometries in detail we have performed B3LYP/6-311G* calculations for the internal rotation with the dihedral angles ∠C−O−O−Cl for CH_3OOCl and ∠C−O−Cl−O for CH_3OClO as reaction coordinates, respectively.

TABLE 1: Harmonic Vibrational Frequencies (in cm^{-1}) of CH_3OOCl, CH_3OClO, and the Transition States for the System CH_3O and ClO Obtained from the DFT Calculations

CH_3OOCl	3155, 3131, 3044, 1510, 1480, 1454, 1207, 1170, 948, 876, 585, 481, 336, 200, 148
CH_3OClO	3133, 3111, 3029, 1519, 1477, 1455, 1180, 1172, 994, 931, 534, 397, 273, 157, 95
TS1	3223, 3102, 1737, 1479, 1357, 1290, 1231, 1145, 1075, 747, 616, 514, 327, 198, 448i
TS2	3030, 2941, 1810, 1532, 1309, 1242, 1222, 1050, 703, 593, 434, 419, 349, 150, 820i

The results of the calculations for the internal rotation are shown in Figures 2 and 3. For CH_3OOCl we found the global minimum to be a gauche conformer with a dihedral angle of 87.5° close to the values of 88.7° (MP2/6-31G(d,p)) and 89.4° (QCISD/6-31G(d,p)) given by Jungkamp et al.[14] Interestingly, the trans structure ($\angle$C−O−O−Cl = 180°) is found 5.8 kcal/mol higher than the gauche structure, while the cis conformer is calculated 12.3 kcal/mol above the global minimum. Thus CH_3OOCl must be considered as a rigid molecule with relatively high barriers for the internal rotation. On the other hand for CH_3OClO the lowest-energy structure (also gauche orientated) is calculated with a dihedral angle C−O−Cl−O of 59.0°, again in agreement with the 58.1° (MP2/6-31G(d,p)) of reference.[14] For this molecule the cis structure is found to lie very close in energy (only 1.8 kcal/mol above the gauche conformer) and the trans conformer is found only 6.9 kcal/mol higher than the global minimum.

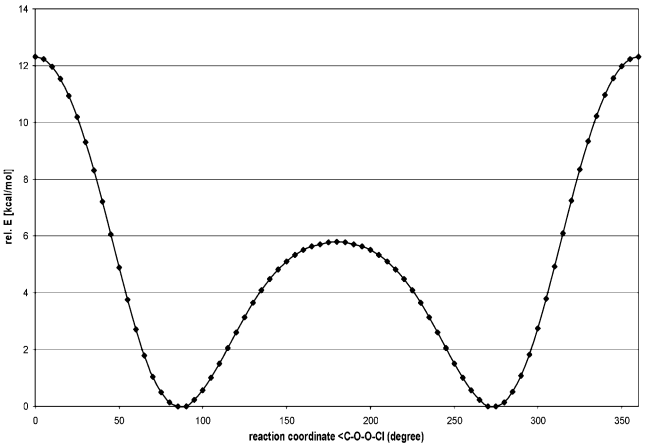

Figure 2. Calculated energy profile at the B3LYP/6-311G* level for the internal rotation of CH_3OOCl. The reaction coordinate is the dihedral angle C−O−O−Cl in degrees.

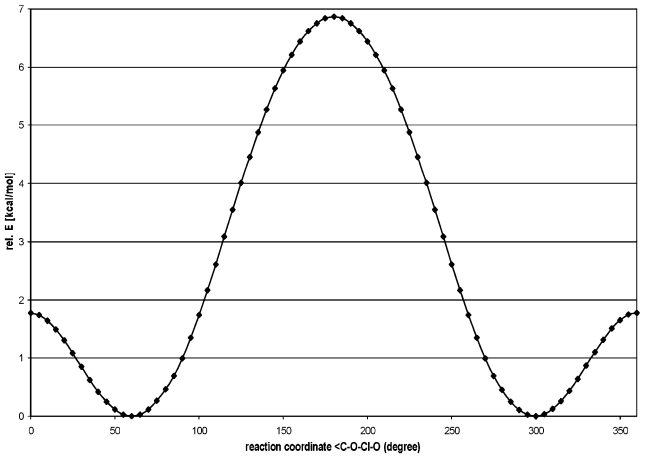

Figure 3. Calculated energy profile at the B3LYP/6-311G* level for the internal rotation of CH_3OClO. The reaction coordinate is the dihedral angle C−O−Cl−O in degrees.

In Table 2 we present the relative stabilities of both species at various levels of theory. As can be seen, CH_3OOCl is about 25 kcal/mol lower in energy than CH_3OClO. We note, however, that the calculated energy difference depends very much on the basis set. This is also found by Jungkamp et al.[14] on the basis of their MP4- and G2-calculations.

Generally the geometries calulated at the DFT level are obtained in reasonable agreement with what is known in the literature.[15,16] For example for CH_3O Höper et al.[16] have performed intensive theoretical studies investigating the Jahn−Teller effect. Their MRCI-optimizations lead to a C−O bond length of 1.393 Å for the C_s symmetric minimum, while we have calculated bond lengths of r(C−O) = 1.369 Å (B3LYP/6-311G*) and r(C−O) = 1.393 Å (RCCSD(T)/cc-pVTZ). As can be seen, the value calculated with B3LYP is found to be about 0.03 Å too short. For the H−C−O angle, Höper et al. calculated 105.3° (MRCI). With DFT and coupled cluster level of theory we found the same value.

The optimized structures of the other species are also in reasonable agreement with analogous results in the literature,[17]and for this reason they are not included in Figure 1.

For the system CH_3O + ClO we have investigated the following reaction pathways:

$$CH_3O + ClO \rightarrow CH_2O + HOCl \quad (2)$$

$$\rightarrow CH_3OOCl \quad (3)$$

$$\rightarrow CH_3OClO \quad (4)$$

$$CH_3OOCl \rightarrow CH_3O_2 + Cl \quad (5)$$

$$\rightarrow CH_2O_2 + HCl \quad (6)$$

$$\rightarrow CH_2O + HOCl \quad (7)$$

$$CH_3OClO \rightarrow CH_3 + ClOO \quad (8)$$

$$\rightarrow CH_3OCl + O \quad (9)$$

Figure 4 presents the relative stabilities based on coupled cluster (CCSD(T)) calculations. The products CH_2O and HOCl are calculated 77 kcal/mol lower in energy than the educts CH_3O and OCl. The corresponding reaction 2 can be described as a hydrogen abstraction by the oxygen atom of the ClO radical. For this abstraction no transition state and thus no energy barrier could be found. This is in agreement with previous results on similar H-abstractions, for example for the $CH_3O + Cl \rightarrow CH_2O + HCl$ reaction which also occurs without an energy barrier.[4] Therefore this reaction 2 will form a very important reaction channel for the system CH_3O and ClO as suggested by Daele et al.[3]

Very interesting are the formations of CH_3OOCl (reaction 3) and CH_3OClO (reaction 4), which are the adducts of CH_3O and ClO. Both molecules are found to be lower in energy than the educts (−27.6 kcal/mol for CH_3OOCl and −5.1 kcal/mol for CH_3OClO) and thus could be considered as a sink for ClO on the ground-state surface. Jungkamp et al.[14] found an energy of formation of 28 kcal/mol for CH_3OOCl based on a mixture of their G2 calculations and of tabulated heats of formation. The formation reactions are found without any barrier. Thus, in addition to the dominant formation of CH_2O and HOCl, especially the reaction to CH_3OOCl will also play an important role.

TABLE 2: Calculated Relative Stabilities in kcal/mol of the Isomers CH_3OOCl and CH_3OClO at Different Theoretical Levels[a]

ΔE	MP2/ 6-311G*	B3LYP/ 6-311G*	CCSD(T)/ cc-pVTZ	MRD-CI+Q/ cc-pVTZ+sp	MP4/ 6-311+G(d,p)[b]	MP4/ 6-311G(d,p)[b]
CH_3OOCl	0.0	0.0	0.0	0.0	0.0	0.0
CH_3OClO	23.6	25.9	22.6	17.3	23.1	27.3

[a] The methods and basis sets are described in the computational techniques. [b] Taken from ref 14.

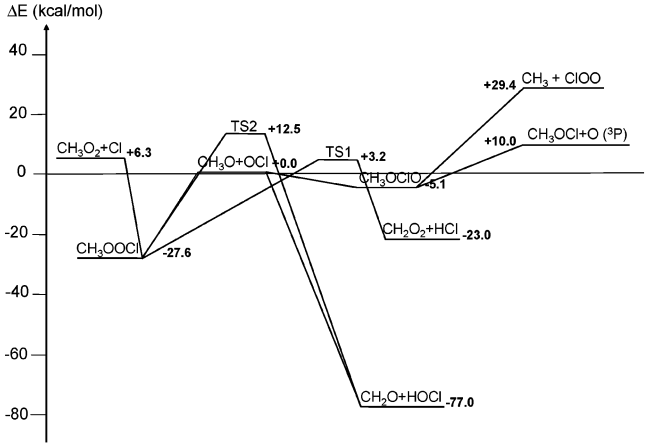

Figure 4. Calculated energy profile (CCSD(T)/cc-pVTZ) of different reaction pathways for the system CH_3O + ClO.

Both adducts are found to be local minima without imaginary frequencies (see Table 1). A conceivable reaction 5 into CH_3O_2 and Cl requires an energy of 33.9 kcal/mol. Therefore, this reaction will not play an important role for the system CH_3O + ClO. But it is worth mentioning that the reverse reaction CH_3O_2 + Cl to CH_3OOCl is thermodynamically favored and found to be without any barrier. Thus CH_3OOCl can also be suggested as a sink for chlorine atoms.

Another pathway is reaction 6 forming CH_2O_2 and HCl from CH_3OOCl. For this reaction we found a transition state (TS1). The reaction is hindered by a barrier of 30.8 kcal/mol. Looking at the transition state TS1 (Figure 1) the Cl−O bond is already elongated from 1.699 Å in CH_3OOCl to 2.796 Å. In addition, the bond between the carbon atom and the H_1 that will be abstracted is elongated from 1.092 Å (in CH_3OOCl) to 1.215 Å. The H−Cl distance is found with 1.760 Å compared to 1.290 Å in molecular HCl. Jungkamp et al.[14] found a quite similar transition state with r(Cl−O) = 2.690 Å, r(H_1−C) = 1.390 Å (thus clearly more elongated than in our calculations), and r(H−Cl) = 1.690 Å based on their MP2 calculations. They also calculated an energy barrier which is only slightly lower than ours. Because of the barrier in reaction 6 above the energy of the initial compounds is also not expected to dominate the kinetics of the investigated system.

According to our calculations, the reaction 7 into CH_2O and HOCl is hindered by an energy barrier of 40 kcal/mol relative to CH_3OOCl. The transition state (TS2) is given in Figure 1. The O−O bond is elongated from about 1.5 Å in CH_3OOCl to 1.935 Å. In addition the C−O distance in TS2 is found to be 1.302 Å and thus approximately 0.1 Å shorter than in CH_3OOCl due to the increasing double bond character in CH_2O. The imaginary frequency of −819.9 cm^{-1} characterizes this stationary point as a first-order saddle point and thus as transition state.

Consequently, on the ground-state energy surface the formation of CH_3OOCl from CH_3O + ClO and from CH_3O_2 + Cl is energetically favored, but further progression into products is hindered by energy barriers. For CH_3OClO we have investigated reactions 8 and 9 where the products are higher in energy.

TABLE 3: Calculated Vertical Excitation Energies of CH_3OOCl and CH_3OClO Calculated with the cc-pVDZ+sp Basis Set as Described in the Computational Techniques[a]

	CH_3OOCl			CH_3OClO		
state	excitation	ΔE [eV]	f	excitation	ΔE [eV]	
X^1A	$(13a)^2$	0.0		$(13a)^2$	0.0	
2^1A	13a → 14a 13a → 15a	3.45 (3.50)	0.00027	13a → 14a	2.56 (2.86)	0.00025
3^1A	12a → 14a 12a → 15a	4.73 (4.81)	0.0023	12a → 14a	4.76 (4.93)	0.0021
4^1A	11a → 14a 11a → 15a	4.80 (4.94)	0.145	13a→15a 11a→14a	5.08 (5.29)	0.086

[a] The excitation energies given in parentheses correspond to calculations using the larger cc-pVTZ+sp basis set.

Therefore, the formation of CH_3OClO from CH_3 + ClOO and from CH_3OCl + O via simple additions are very probably on the ground-state potential surface.

To allow further conclusions about the function of CH_3OOCl and CH_3OClO as sink for chlorinated radicals such as ClO one also has to consider the excited states of the molecules and their stabilities against photodissociation in order to understand their photochemistry.

Table 3 presents a comparison of the computed electronic excitation energies between CH_3OOCl and CH_3OClO calculated with the cc-pVDZ+sp and the larger cc-pVTZ+sp basis set. Changes in this energy range are less than 0.3 eV between both basis sets. But it is also obvious that the basis set influence is much more important for CH_3OClO than for CH_3OOCl. The electronic absorption spectra have been studied neither theoretically nor experimentally until now. The ground states of both molecules are singlet states. The corresponding triplet state is calculated 65 kcal/mol (MRD-CI+Q) above the singlet ground state for CH_3OOCl and 59 kcal/mol (MRD-CI+Q) for CH_3OClO.

The HOMO−LUMO excitation (13a → 14a) of CH_3OOCl is calculated at 3.50 eV with only a small oscillator strength. In Figure 5 the charge density contours of characteristic valence orbitals (11a, 12a, 13a) and the LUMO 14a of CH_3OOCl and CH_3OClO are given. As can be seen, the HOMO 13a can be described to consist of a linear combination of π^*(O2−Cl), π^*(O1−O2), and σ(C−O) bonding and has thus little stabilizing character. On the other hand, the LUMO 14a mainly consists of a dominant σ^*(O2−Cl) antibonding part. Therefore, in a simple picture, the HOMO−LUMO excitation 13a → 14a can be reduced to a π^*(O2−Cl) → σ^*(O2−Cl) transition for which normally quite small oscillator strengths as computed here are obtained.

At 4.81 eV we have calculated the transition 12a → 14a. As can be seen from Figure 5 the MO 12a is dominated by a chlorine 3p-lone pair which is orientated tangentially. The MO is stabilized by a σ(O1−O2) bond. The transition 12a → 14a can be reduced to an n(Cl) → σ^*(O2−Cl) excitation for which again a relatively small oscillator strength is found.

The excitation 11a → 14a is calculated at 4.94 eV with a large f-value of 0.145. The MO 11a is clearly π^*(C−O1) and π^*(O1−O2) antibonding with a dominant σ(O2−Cl) bonding character. Therefore, this excitation mainly consists of a σ(O2−

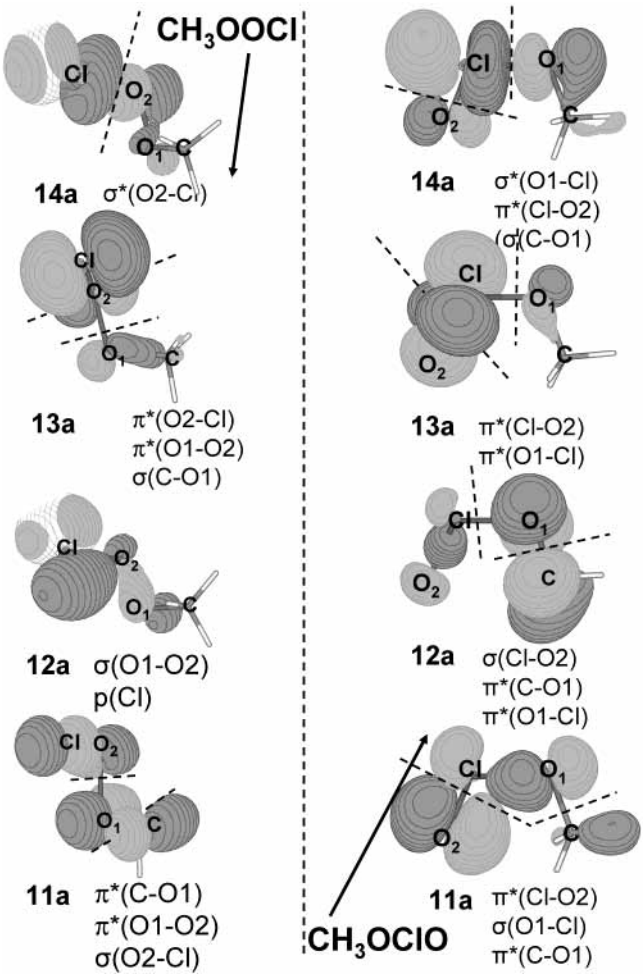

Figure 5. Charge density contours of characteristic occupied valence orbitals (11a, 12a, 13a) and the lowest virtual molecular orbital LUMO (14a) of CH_3OOCl and CH_3OClO based on MCSCF calculations.

Cl) → σ*(O2−Cl) transition for which the relatively strong *f*-value can be understood. In addition, this strong transition could possibly help to detect the molecule in field and laboratory measurements concerning atmospheric chemistry.

For CH_3OClO the first transition corresponds to the HOMO−LUMO excitation 13a → 14a at 2.86 eV with an only small oscillator strength leading to the first excited state 2^1A. The HOMO 13a of CH_3OClO is dominated by π*(Cl−O2) antibonding character localized at the outer Cl−O bond and some π*(O1−Cl) antibonding character localized at the inner Cl−O bond. The LUMO 14a can be described to be π*(Cl−O2) antibonding at the outer O−Cl bond and σ*(O1−Cl) antibonding at the inner Cl−O bond. Therefore, in a simple picture, the HOMO−LUMO excitation can be reduced to a transition corresponding to π*(Cl−O2)→ π*(Cl−O2) and π*(O1−Cl)→ σ*(O1−Cl) excitations for which the relatively small oscillator strength can be understood.

The excitation 12a → 14a leads to the 3^1A state calculated at 4.93 eV with an oscillator strength of 0.003. The MO 12a consists of σ(Cl−O2), π*(O1−Cl), and dominant π*(C−O) characters. Thus the 12a → 14a transition can be understood as a combination of σ(Cl−O2)→ π*(Cl−O2)−, π*(O1−Cl)→ σ*-(O1−Cl)−, and π*(C−O)→ σ(C−O) transitions. Consequently, the calculated oscillator strength for this transition is larger than for the HOMO−LUMO excitation.

At 5.29 eV we have calculated the 4^1A state corresponding to a 13a → 15a and 11a → 14a excitation. The MO 11a can be described as a combination of π*(Cl−O2) contributions at the outer Cl−O bond and a very dominant σ(Cl−O) part. The virtual MO 15a has Rydberg character. Thus the transition 13a → 15a corresponds to an excitation into a diffuse virtual MO (this kind of transitions usually has quite small oscillator strength). On the other hand the transition 11a → 14a can be mainly reduced to a σ(O−Cl)→ σ*(O−Cl) excitation for which normally relatively large oscillator strengths are computed. Therefore the size of the oscillator strength calculated for the transition under investigation can be understood by the combination mentioned above. The stronger transitions computed at 5.29 eV for CH_3OClO and at 4.94 eV for CH_3OOCl could give a hint for future spectroscopic search.

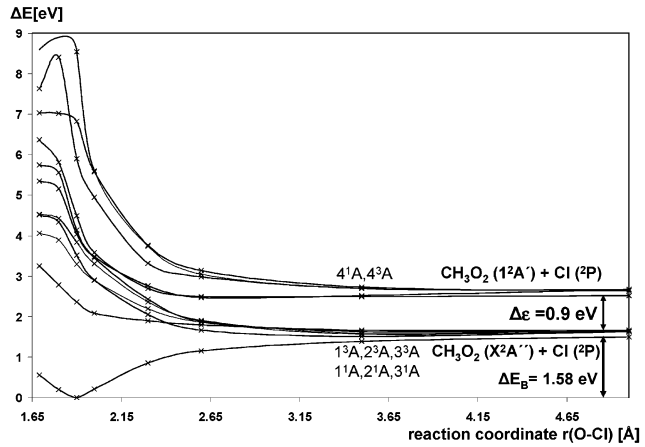

Figure 6. Calculated potential energy curve for O−Cl photodissociation of CH_3OOCl.

4. Photodissociative Studies

In Figure 6 we present the potential energy curves calculated for the lowest eleven states for O−Cl dissociation. The lowest excited triplet states of CH_3OOCl are also included in the study. The ground state of CH_3OOCl is a singlet state, and thus, because of spin conservation, transitions to singlet excited states are the most likely processes for photoinduced dissociation. On the other hand, recent experimental photodissociation studies[18] have shown that spin−orbit coupling is nonnegligible for some chlorine species such as HOCl, and thus weak transitions to excited states could also be possible. Therefore, we included also transitions to triplet states in the present study.

Five excited states (2^1A, 3^1A, 1^3A, 2^3A, 3^3A) with vertical excitation energies between 2.5 and 5 eV are found to be highly repulsive for O−Cl elongation, leading to the first dissociation channel CH_3O_2 (X^2A'') + Cl (X^2P) calculated at 1.58 eV (36.5 kcal/mol) which is in line with the energy difference between CH_3OOCl and CH_3O_2 + Cl of 33.9 kcal/mol calculated at the CCSD(T)/cc-pVTZ level (Figure 4). The repulsive character can be understood on the basis of qualitative MO considerations. As discussed above, the first excited states correspond to excitations into the LUMO 14a which is σ*(Cl−O) antibonding (Figure 5). Thus excitation into this LUMO 14a will lead to a weaker Cl−O bond in CH_3OOCl and consequently Cl−O bond cleavage is possible.

Interestingly, there is a second dissociation channel calculated only 0.9 eV above the first one. This channel corresponds to CH_3O_2 in its first excited state $1^2A'$. We have calculated five excited states that are also repulsive with respect to this second dissociation channel. Additionally, the very strong transition 4^1A ← X^1A leads to the second dissociation channel as well. Thus photodissociation via Cl−O cleavage is very probable because

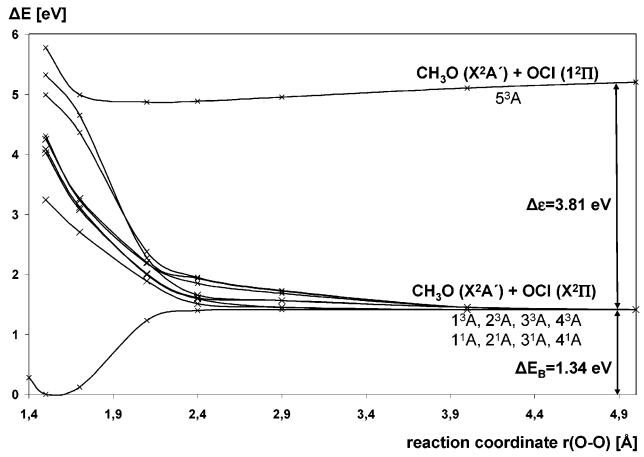

Figure 7. Calculated potential energy curve for O−O photodissociation of CH_3OOCl.

we have computed 10 repulsive excited states with excitation energies between 2.5 and 9 eV.

The results for the second model adopted for the potential energy curves, i.e., the elongation of the O−O bond as reaction coordinate, are displayed in Figure 7. It is seen that for this cleavage we find seven excited states that are highly repulsive in the enery region between 2.5 and 5 eV. These seven excited states correlate with the first dissociation channel of CH_3O (X^2A', $1^2A''$, due to Jahn−Teller distortion) and ClO ($X^2\Pi$) together with the ground state. The first dissociation channel is calculated at 1.34 eV (30.9 kcal/mol), which is again in line with the energy difference between CH_3OOCl and $CH_3O + ClO$ of 27.6 kcal/mol calculated at the coupled cluster level (Figure 4). Again the repulsive character can be explained using MO considerations. The LUMO 14a is not only σ^*(Cl−O) antibonding but shows some antibonding π^*(O−O) contributions as can be seen from Figure 5. Thus excitations into the LUMO 14a lead not only to a weaker Cl−O bond in CH_3OOCl but also to a weakening of the O−O bond.

5. Summary and Conclusions

We have investigated pathways on the potential energy surface of the system CH_3O and ClO. Experimentalists[3] have suggested the formation of CH_2O and HOCl (reaction 2) to be the major reaction of the system CH_3O and ClO. Other products such as CH_2O_2 and HCl (reaction 2a) have not been detected. Our theoretical study suggests that the system is dominated by two reactions. The hydrogen abstraction from the methoxy radical under formation of CH_2O and HOCl (reaction 2) is found to be barrier free and therefore very important. This finding is in line with the experimental results. In addition, there are two low-lying adducts, CH_3OOCl and CH_3OClO, whose formations (reactions 3 and 4) are also calculated without a barrier. These molecules are found to be asymmetric with dihedral angles of $\angle C-O-O-Cl = 87.5°$ and $\angle C-O-Cl-O = 59.0°$ (gauche conformers). Further decomposition of the low-lying CH_3OOCl is found to be thermodynamically not favored since it is hindered by energy barriers in the order of 30−40 kcal/mol. Therefore, on the ground-state potential energy surface these molecules may act as a possible sink for chlorinated radicals such as ClO. Since CH_3OOCl is about 25 kcal/mol lower in energy than CH_3OClO, we expect that reactions 2 and 3 will be the main channels for the reactive system $CH_3O + ClO$.

In addition we have performed MRD-CI studies of the excited states of the adducts CH_3OOCl and CH_3OClO. For CH_3OOCl we found a dominant transition at 4.80 eV corresponding to a σ(Cl−O2)−σ^*(Cl−O2) excitation. For the other adduct CH_3OClO we calculated a relatively strong transition at 5.08 eV, which can guide future spectroscopic search.

Since CH_3OOCl is about 25 kcal/mol lower in energy than CH_3OClO, we have concentrated our photodissociative studies on the more stable isomer. For the photodissociation of CH_3OOCl via Cl−O and O−O cleavage, we found the lower-lying excited states to be highly repulsive, leading to dissociation channels of the products in their ground and first excited states. Thus, photodissociation of CH_3OOCl into CH_3O_2 and Cl on one hand and CH_3O and ClO on the other hand is very probable. Consequently, CH_3OOCl can act as a sink in its ground state, but under photodissociation the decomposition is favored.

These results are in line with our findings[4,6] for the system CH_3O+Cl where the reaction channel forming CH_2O and HCl is most favored. In addition, the formation of the low-lying adducts methyl hypochlorite CH_3OCl and chloromethanol CH_2ClOH is very dominant and thus CH_2ClOH can be seen as a sink for chlorine atoms on the ground-state surface. But similar to CH_3OOCl, chloromethanol is also found to be unstable against photodissociation into CH_3O and Cl.

As a conclusion, one finds that the methoxy radical CH_3O can act as a sink for ClO and Cl on the ground-state surface under formation of CH_3OOCl, CH_2ClOH, and CH_3OCl. But both adducts are found to be unstable against photodissociation.

Acknowledgment. The present study is part of a NATO science project "Study of elementary steps of radical reactions in atmospheric chemistry". The financial support from the NATO grant is gratefully acknowledged. M.S. acknowledges a grant from the "Fonds der Chemischen Industrie". M. Hanrath is thanked for various improvements of the DIESEL program package.

References and Notes

(1) De More, W. B.; Sander, S. P.; Golden, D. M.; Hampson, R. F.; Kurylo, M. J.; Howard, C. J.; Ravishankara, A. R.; Kolb, C. E.; Molina, M. J. *Chemical Kinetics and Photochemical Data for Use in Stratospheric Modeling*, Jet Propulsion Laboratory, Pasadena, California, **1992**, JPL Publication 92-20.

(2) Frost, M. J.; Smith, I. W. M. *J. Chem. Soc., Faraday Trans.* **1990**, 86, 1751 and 1757.

(3) Daele, V.; Laverdet, G.; Poulet, G. *Int. J. Chem. Kinet.* **1996**, 28, 589−598.

(4) Drougas, E.; Kosmas, A. M.; Schnell, M.; Mühlhäuser, M.; Peyerimhoff, S. D. *Mol. Phys.* **2002,** 100, 2653−2658.

(5) Helleis, F.; Crowley, J.; Moortgart, G. *Geophys. Res. Lett.* **1994**, 21, 1795−1798.

(6) Mühlhäuser, M.; Schnell, M.; Peyerimhoff, S. D. *Mol. Phys.* **2002**, 100, 509−515.

(7) Frisch, M. J.; Trucks, G. W.; Schlegel, H. B.; Scuseria, G. E.; Robb, M. A.; Cheeseman, J. R.; Zakrzewski, V. G.; Montgomery, J. A., Jr.; Stratmann, R. E.; Burant, J. C.; Dapprich, S.; Millam, J. M.; Daniels, A. D.; Kudin, K. N.; Strain, M. C.; Farkas, O.; Tomasi, J.; Barone, V.; Cossi, M.; Cammi, R.; Mennucci, B.; Pomelli, C.; Adamo, C.; Clifford, S.; Ochterski, J.; Petersson, G. A.; Ayala, P. Y.; Cui, Q.; Morokuma, K.; Malick, D. K.; Rabuck, A. D.; Raghavachari, K.; Foresman, J. B.; Cioslowski, J.; Ortiz, J. V.; Stefanov, B. B.; Liu, G.; Liashenko, A.; Piskorz, P.; Komaromi, I.; Gomperts, R.; Martin, R. L.; Fox, D. J.; Keith, T.; Al-Laham, M. A.; Peng, C. Y.; Nanayakkara, A.; Gonzalez, C.; Challacombe, M.; Gill, P. M. W.; Johnson, B. G.; Chen, W.; Wong, M. W.; Andres, J. L.; Head-Gordon, M.; Replogle, E. S.; Pople, J. A. *Gaussian 98*; Gaussian, Inc.: Pittsburgh, PA, 1998.

(8) MOLPRO 2000 is a package of ab initio programs written by Werner, H.-J.; Knowles, P. J.

(9) Dunning, T. H., Jr.; *J. Chem. Phys.* **1989**, 90, 1007. (b) Woon, D. E.; Dunning, T. H., Jr. *J. Chem. Phys.* **1993**, 98, 1358.

(10) Mühlhäuser, M.; Schnell, M.; Peyerimhoff, S. D. *Mol. Phys.* **2002**, 100, 509. (b) Schnell, M.; Mühlhäuser, M.; Peyerimhoff, S. D. *J. of Mol. Spectrosc.* **2002**, 214, 124. (c) Schnell, M.; Mühlhäuser, M.; Peyerimhoff, S. D. *Chem. Phys. Lett.* **2002**, 361, 1.

(11) Hanrath, M.; Engels, B. *Chem. Phys.* **1997**, 225, 197.

(12) Hanrath, M.; private communication.

(13) Buenker, R. J.; Peyerimhoff, S. D. *Theor. Chim. Acta* **1974,** 35, 33. (b) Buenker, R. J.; Peyerimhoff, S. D. *Theor. Chim. Acta* **1975**, 39, 217.

(14) Jungkamp, T. P. W.; Kukui, A.; Schindler, R. N. *Ber. Bunsen-Ges. Phys. Chem.* **1995**, *99*, 1057−1066.

(15) Francisco, J. S. *Int. J. Quantum Chem.* **1999**, 73, 29.

(16) Höper, U.; Botschwina, P.; Köppel, H. *J. Chem. Phys*. **2000**, 112, 4132.

(17) Herzberg, G.; *Molecular Spectra and Molecular Structure, II. Spectra of Polyatomic Molecules*; Van Nostrand Reinhold: New York, 1966. (b) He, T.-J.; Chen, D.-M.; Lin, F.-C.; Sheng, L.-S. *Chem. Phys. Lett.* **1994**, 21, 1795. (c) Herzberg, G.; *Molecular Spectra and Molecular Structure, I. Spectra of Diatomic Molecules*; Van Nostrand Reinhold: New York, 1950.

(18) Barnes, R. J.; Lock, M.; Coleman, J.; Sinha, A. *J. Phys. Chem. A* **1996**, 100, 453. (b) Francisco, J. S.; Hand, M. R.; Williams, I. H. *J. Phys. Chem. A* **1996**, 100, 9250.